Cell properties of nucleus pulposus progenitor cells declines with intervertebral disc degeneration

Xiao-Chuan Li[1,2], Xue-Dong Bai[1], Hong-Kui Xin[1], Ying-Wei Bai[1,3], Shi Cheng[1], Tian-Yong Wen[1], Shi-Sheng Pei[1], Jing-Wei Ying[1], De-Li Wang[1], Qing He[1] and Di-Ke Ruan[1]

[1]Department of Orthopaedic Surgery, Navy General Hospital, Beijing, 100048, China

[2]Department of Orthopaedic Surgery, Gaozhou People's Hospital, Guangdong, 525200, China

[3]Department of Orthopaedic Surgery, The Third People's Hospital of Huizhou, Guangdong, 516000, China

Correspondence to: Di-Ke Ruan, **email:** ruandikengh@163.com

Keywords: *intervertebral disc, nucleus pulposus progenitor cells, cell properties, cell senescence, regenration medicine*

Received: *August 09, 2017* ***Accepted:*** *September 20, 2017* ***Published:*** *December 07, 2017*

ABSTRACT

Endogenous repair of nucleus pulposus progenitor cells (NPPCs) has exhibited encouraging regenerative potential for treating intervertebral disc degeneration (IDD). However, few studies have explored the properties of NPPCs during the progression of IDD. Hence, additional studies are needed to characterize NPPCs from human degenerated intervertebral disc (IVDs) at different Pfirrmann grades. In this study, human NPPCs were isolated and identified from human IVDs with different Pfirrmann grades. Then, cell biological characteristics, including proliferation, colony formation, cell senescence, migration capacity and chondrogenic ability, were compared. NPPCs were successfully harvested from grade I to IV IVDs, but not from grade V IVD due to the marked loss of nucleus pulposus tissue at grade V, leading to poor cell cultures. All four grades of NPPCs were identified as mesenchymal stem cells (MSCs) based on the criteria of the International Society for Cellular Therapy (ISCT) and shared similar cell morphological characteristics. In addition decreasing trends in proliferation, colony-formation capacity, migration, and chondrogenic ability and increasing levels of cell senescence; were detected in cells from grade I to IV IVDs, with significant changes between NPPCs of grade II and III. In summary, compared with NPPCs from normal IVDs (grade I), cells from degenerated IVDs (grades II to IV) exhibited gradually decreased cell properties and increased cell senescence. Grade II NPPCs displayed the optimal regeneration potential, suggesting that these NPPCs are an ideal candidate for endogenous repair of IDD.

INTRODUCTION

Intervertebral disc degeneration (IDD), as the main pathological basis of back pain, urgently requires more effective fundamental therapies rather than symptom relief [1]. As the population ages, the number of people suffering from IDD is expected to grow exponentially and place a heavy burden on healthcare resources in the near future [2]. Although stem cells (SCs) display encouraging capabilities for self-renewal and multilineage differentiation [3], exogenous SCs often do not survive the harsh environment of IDD, which includes strong force, acidic pH, hypoxia, hyperosmolarity and limited nutrients [4]. Hence, the regeneration potential of endogenous cells, such as nucleus pulposus progenitor cells (NPPCs), gaining increasing attention for potential applications in new treatments for IDD.

Endogenous tissue repair, based on the regeneration ability of tissue-specific SCs, has been verified in most human tissues, including liver, skin, muscle, nervous

system, heart, and bone [5]. NPPCs, a newly discovered type of endogenous intervertebral disc (IVD) SCs, have been characterized in mouse, rabbit, porcine, canine, rhesus monkey and both healthy and degenerating human IVDs [6–10]. In clinical practice, spine surgery patients treated with a dynamic fixation system occasionally display regeneration phenomena in operated segments [11], while experimentally, NPPCs exhibit superior performance in surviving adverse environments [12–14]. However, recent reports have indicated that NPPCs gradually become exhausted with increased age and progressive degeneration in IDD [15–17].

Our previous work also revealed distinct differences between young and old mice in the properties of NPPCs, including their cell proliferation ability, colony-forming rate and cell senescence [18]. However, whether the biological characteristics of NPPCs decrease with increasing degeneration in IDD remains unclear. We hypothesized that pathological changes during IDD may be accompanied by a decline in NPPC properties and cell regeneration potential. Therefore, in the present work, we tested this hypothesis and explored the optimal regeneration window for treating IDD. NPPCs from lumbar spine surgery patients with different Pfirrmann grades were harvested and identified based on the criteria of mesenchymal stem cells (MSCs) established by an expert panel from the International Society for Cellular Therapy (ISCT) [19]. Subsequently, cell morphology and cell properties such as cell proliferation, colony-forming ability, cell senescence and migration ability were analyzed. In addition, chondrogenic induction ability was also assessed with a pellet culture protocol by measuring pellet weight and functional gene/protein expression levels. Our findings offer new insights into potential biological therapies and suggest a new regeneration strategy for promoting regeneration in IDD.

RESULTS

Representative MRI scans and gross morphology of NP tissue

Representative MRI scans of patient IVDs of different Pfirrmann grades (grades I to IV) are shown in Figure 1A, and the gross morphology of the nucleus pulposus (NP) tissue is accordingly shown in Figure 1B. As the Pfirrmann grade gradually increased from I to IV, the NP tissue subsequently changed from translucent to opaque in grades I and II, with signs of dehydration in grade III and finally fibrosis in grade IV.

Cell morphology and growth characteristics

After primary cells were cultured and harvested at a low density of 500 cells/ml for colony formation screening, passage 1 (P1) NPPCs were obtained as colonies in a compact type and rounded structure after 2 weeks. As upon reaching 60–70% confluence, the cells were subcultured and proliferated until P9. Morphologically, P3 NPPCs exhibited homogeneous elongated spindle shapes and compact parallel or vortex populations (Figure 2A). In addition, the proliferation capacities of P3 cells assessed by CCK-8 assay displayed similar cell growth curves, all displaying an 'S' shape after 13 days of culture (Figure 2B). However, various differences were detected in P9 cells, which exhibited a larger volume and more-slender tentacles (Figure 2A). In addition, less compact cell arrangements were also found, with the highest proliferation ability observed in grade I cells at days 7, 9, 11 and 13 (Figure 2C). Moreover, markedly lower OD values were observed in grade III and IV groups compared with grade II on days 11 and 13 (Figure 2C).

Phenotypic characteristics and multilineage differentiation potential of NPPCs

In multilineage differentiation tests, all four grades of cells were capable of osteogenic, chondrogenic and adipogenic differentiation in three types of differentiation media after 3 weeks of induction (Figure 3A). For phenotypic characterization, the expression levels of SC surface markers were analyzed using flow cytometry: all four grades of cells were positive for CD73, CD90, and CD105 expression (> 95%) and negative for the hematopoietic progenitor cell marker CD34, the leukocyte common antigen CD45, and the immune marker HLA-DR (< 2%, Figure 3B and 3C). In summary, the obtained SCs met the ISCT criteria for MSCs, including adhesive characteristics, SC phenotypic expression and multilineage differentiation potential.

Colony-forming ability

When cultured at a low density of 500 cells/ml, all four types of P3 NPPCs (grades I to IV) were able to form fibroblastic colonies, with colony diameters ranging from 0.5 mm to 3 mm (Figure 4A and 4B). In colony formation rate assays, NPPCs displayed a decreasing trend in colony formation rate from grade I to IV. Although grade I cells displayed a slightly high colony-forming rate than grade II, the markedly decreased rates detected for grades III and IV were of great significance, indicating the considerably weaker colony-forming abilities of grade III and IV NPPCs (Figure 4C).

Cell senescence

Cell senescence was analyzed using positive staining for SA-β-gal. SA-β-gal positive staining gradually increased from grade I to IV (Figure 5A). The SA-β-gal positive staining rate significantly increased from grade I to IV, with a slightly higher rate in the grade II group and

markedly higher rate in the grade III and IV groups than in the grade I group (Figure 5B). Moreover, cell senescence-related gene expression levels were analyzed for further comparison. p16 gene expression gradually enhanced from grade I to IV, with much higher expression in grades III and IV. Likewise, p21 and p53 gene expression levels also slightly increased from grade I to IV, with a strong higher expression in grades III and IV (Figure 5D and 5E).

Migration activity of NPPCs from Pfirrmann grade I to IV IVD

Wound-healing assays were performed to compare the migration abilities of NPPCs. After incubation in serum-free DMEM for 24 h, scratched wounds induced ingrades I to IV NPPCs closed to varying extents. Although all four types of cells exhibited migration ability, some differences were detected. The wound-healing potential gradually decreased from grade I to IV, and all the differences tested were significant ($P < 0.05$, Figure 6A and 6B).

Chondrogenic capacity of NPPCs from grade I to IV IVD

A pellet culture protocol was performed to evaluate chondrogenic potential. During chondrogenesis, pellet size is expected to gradually increase in all four groups. However, after 6 weeks of chondrogenic induction, pellet GAG/weight gradually decreased from grades I to IV (Figure 7A and 7E). All four types of NPPCs showed highly positive staining for Alcian blue, indicating the deposition of extracellular matrix (Figure 7B). Regarding the expression levels of chondrogenic genes, both collagen IIα1 and Sox-9 gene expression level decreased from grade I to IV, whereas aggrecan expression levels showed no difference (Figure 7F). In addition, collagen IIα1 and Sox-9 gene expression levels exhibited significantly greater decreases in both grade III and grade IV cells compared with grade I cells, with a slight reduction in grade II cells after 6 weeks of chondrogenic induction (Figure 7F). A similar change in collagen II protein levels was detected via quantitative immunohistochemistry analysis (Figure 6C and 6D).

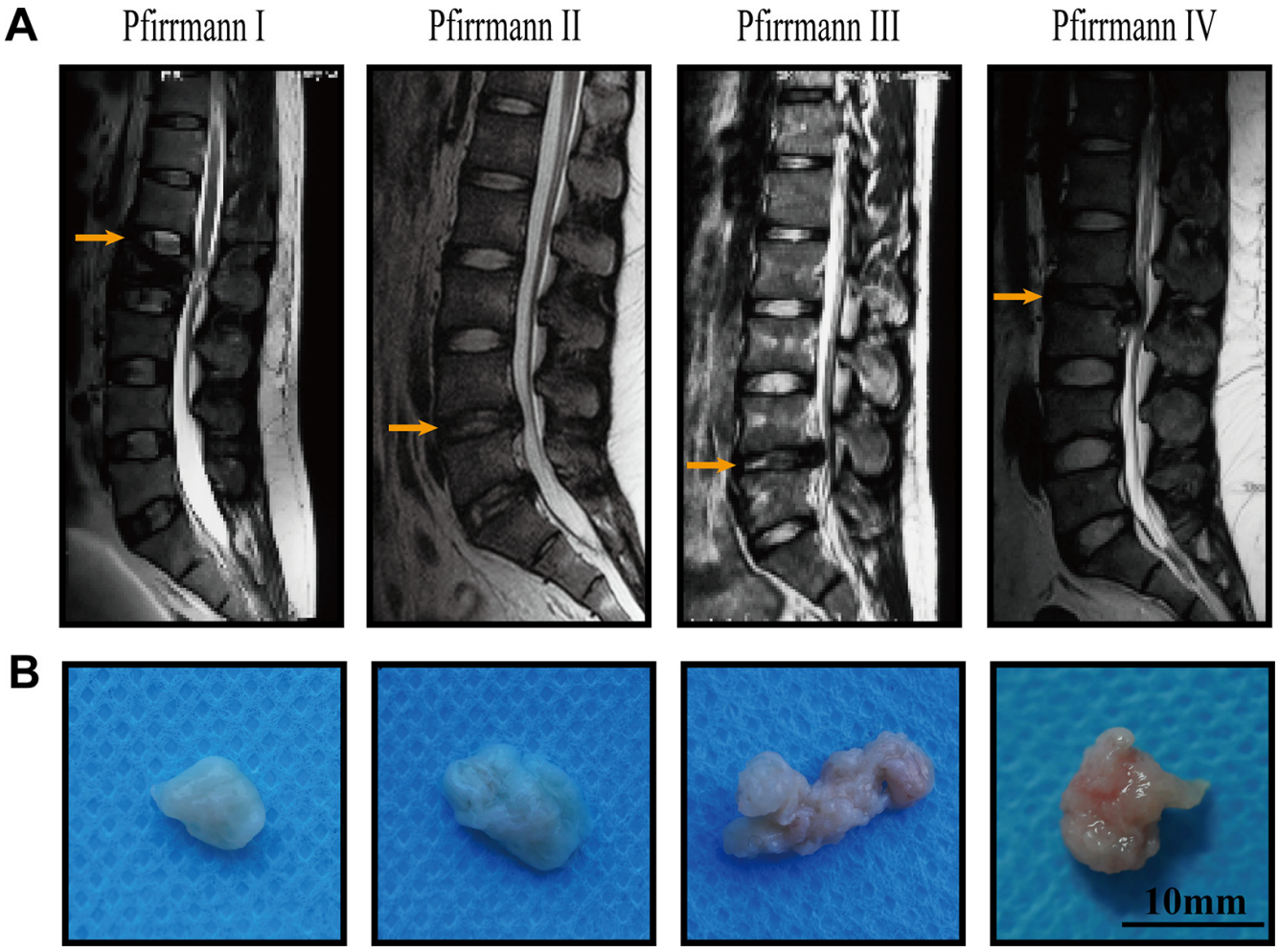

Figure 1: Representative MRI scans and gross morphology of NP tissue from grade I to IV IVDs (**A**) Representative images of lumbar spine MRI from grade I to IV IVDs. (**B**) Representative images of gross morphology of NP tissue from grade I to IV IVDs.

Discussion

The robust repair potential of SCs in many tissues has drawn increased attention for treating IDD [20, 21]. However, the harsh environment in IDD poses a tremendous challenge for exogenous cell survival due to limited nutrition and inflammatory conditions [22]. Several previous reports have shown that endogenous NPPCs exhibit superior potential in IDD regeneration, with better performance in the degenerated disc environment and better tissue-specific properties with lineage conservation potential [23–26]. Therefore, it is of critical importance to further elucidate these phenomena.

Despite the encouraging regeneration potential of NPPCs in normal IVDs, cells from degenerated IVDs remain largely uncharacterized to date [27, 28]. The tissue microenvironment is still thought to play an important role in maintaining SC proliferation and differentiation [29, 30]. In addition, cell properties decrease with age and degeneration during IDD progression [31]. Thus, the present study was performed to assess changes in the biological characteristics and regeneration potential of NPPCs from different IVD state. The Pfirrmann grade system, which is divided into 5 grades, including grades I-V, based on MRI signal intensity, was used to quantify different degeneration degrees of IDD [32]. To the best of our knowledge, this is the first report to provide a side-by-side comparison of NPPCs from grade I to IV IVDs, although grade V IVDs were excluded due to a lack of NP tissue. Our results demonstrated that all four types of NPPCs shared SC biological characteristics but displayed varying cell properties and regeneration potential in the process of IDD.

In the present study, all four grades of NPPCs were identified as SCs according to the criteria of the ISCT and shared similar cell morphologies and characteristics. However, decreasing levels of proliferation, colony-formation capacity, migration, and chondrogenic ability and increasing levels of cell senescence, were detected in NPPCs from grade I to IV IVDs, with significant pathological changes observed between grades II and III. Finally, our results collectively suggest the potential application of grade II NPPCs as an ideal candidate for endogenous repair of IDD.

Several methods have been previously tested for isolating NPPCs, including flow cytometry, agarose suspension culture, and colony screening [15, 25, 33]. In the present study, a mature low-density seeding protocol was adopted to select NPPCs, based on the fact that only tumor cells or SCs can proliferate in a clonal format [25]. Afterward, all selected SCs displayed homogeneous cell morphology at P3, with no significant differences in proliferative potential detected between groups. Finally, the harvested cells were found to exhibit adhesive capacity, SC phenotypic characteristics and multilineage differentiation potential, fulfilling the SC criteria of the ISCT [34].

Although P3 NPPCs of all four grades displayed equal proliferation ability, P9 cells showed considerably decreased proliferation in grades III and IV, accompanied by degenerative changes in cell morphology from grades I

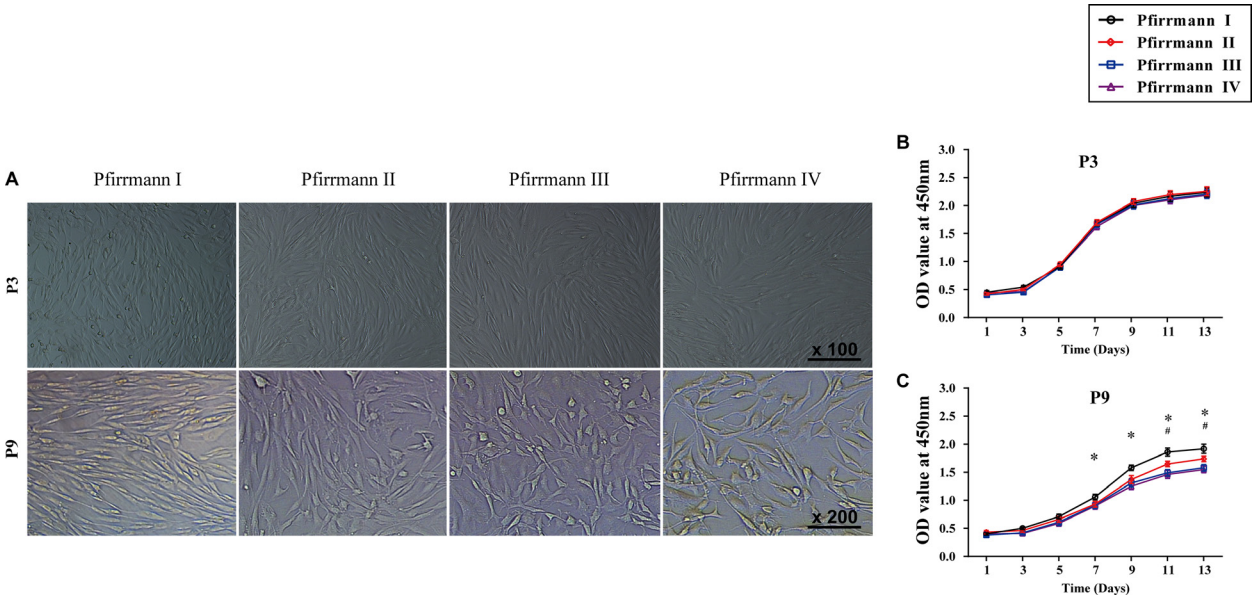

Figure 2: Cell morphology and growth status of NPPCs from grade I to IV IVDs. (**A**) The morphology of P3 and P9 cells was observed under a microscope. (**B**) The growth curves of P3 cells showed similar proliferation abilities and displayed 'S' shapes after 13 days of culture ($n = 3$). (**C**) The growth curves of P9 cells showed a declining proliferation trend from grade I to IV, and higher OD values of grade I at days 7, 9, 11 and 13 were observed compared with those of grade II ($P < 0.05$, $n = 3$). Moreover, significantly lower OD values were detected for grade III than for grade II at days 11 and 13 ($P < 0.05$, $n = 3$). $^{*}P < 0.05$ indicates a significant difference between grades I and II; $^{\#}P < 0.05$ indicates a significant difference between grades II and III.

to IV. These differences in P9 cells from P3 cells may be due to the *in vitro* culture medium providing sufficient nutrition to inhibit the decline of cell proliferation in degenerated NPPCs. As cells undergo increased passaging, slight differences can be magnified and detected. In addition, NP samples also changed from transparent to fibrotic, indicating that the environment in IDD was degenerating. Collectively, these direct changes may indicate the occurrence of cell degeneration consistent with IDD, and this process may be markedly accelerated in grade III and IV IVDs.

Both cell proliferation and colony-forming ability are important cell properties, reflecting cell regeneration potential in tissue engineering. Our results revealed gradual decreases in proliferation and colony-formation rate from grades I to IV, with a marked decline in grade III and IV cells. This result is supported by previous reports that NPPCs from normal IVDs share similar proliferation and colony-forming abilities with bone marrow mesenchymal stem cells (BMSCs), while cells from degenerated IVDs display inferior potential, probably due to the inflammatory effects of degenerated IVDs [35]. On the other hand, with the degeneration of IVDs, endogenous NPPCs are directly stimulated to repair pathological damage by promoting

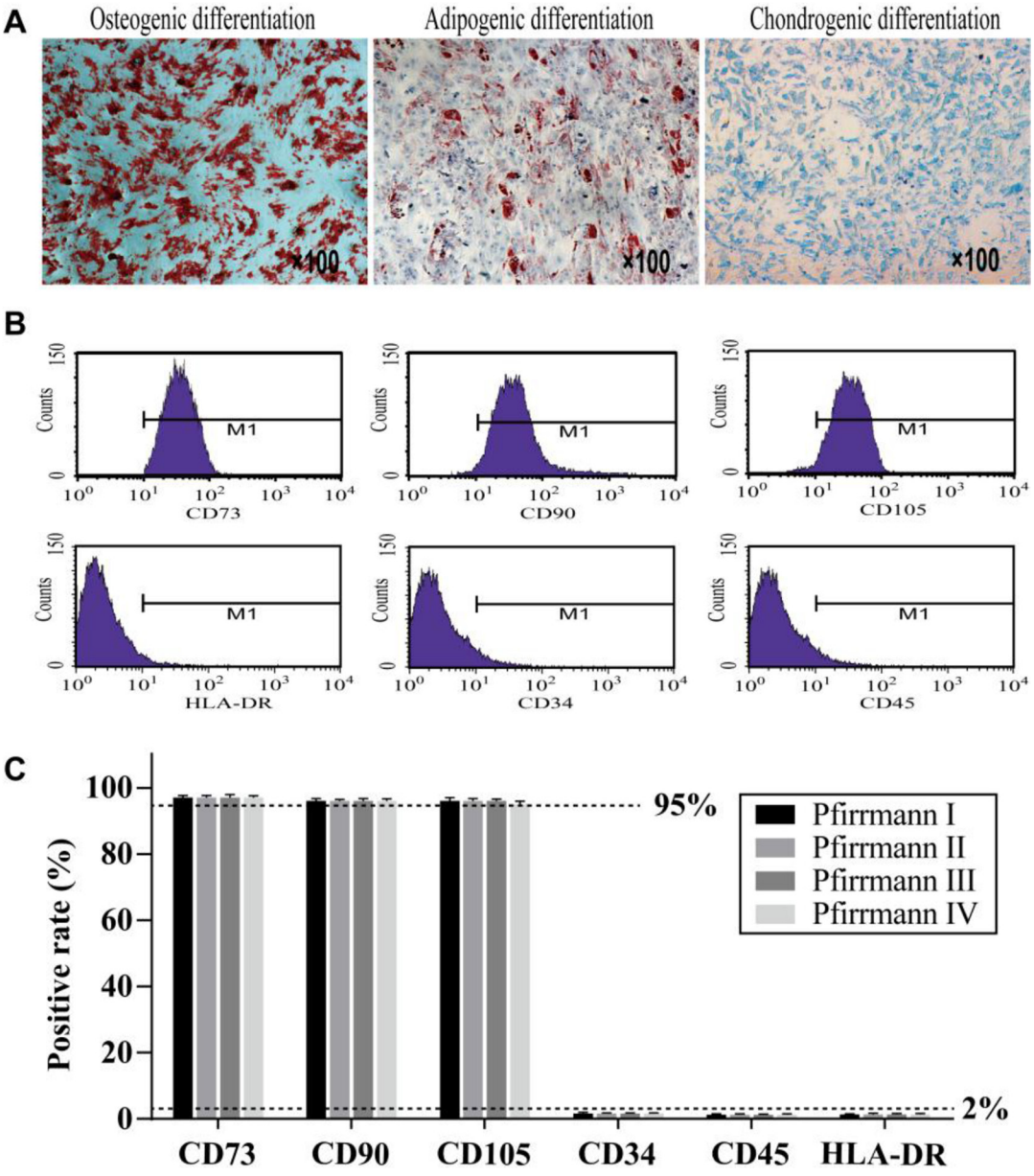

Figure 3: Identification of NPPCs in IVDs from Pfirrmann grades I to IV. (**A**) Representative images of osteogenic, adipogenic, and chondrogenic differentiation positively stained by alizarin red, oil red O and Alcian blue, respectively, indicating three lineage differentiation abilities after 21 days of induction. (**B**) Representative images of positive expression of SC surface markers CD73, CD90, and CD105 and negative expression of CD34, CD45 and HLA-DR. (**C**) Quantitative analysis of immunophenotypic profiles, showing positive expression of CD73, CD90, and CD105 (> 95%, $n = 16$) and negative expression of CD34, CD45 and HLA-DR (< 2%, $n = 16$).

cell proliferation, which would ultimately lead to the exhaustion of their proliferation potential.

Cell senescence, as a key factor in maintaining normal tissue homeostasis, can decrease cell self-repair and regenerative potential [36]. In our study, an increasing percentage of SA-β-gal-positive cells was detected among grade I to IV NPPCs, with a significantly higher increase in the cell senescence rate in both grade III and IV cells. This result was further confirmed by analyzing the gene expression of p16, p21 and p53, corresponding to the p16-pRb and p53-p21-pRb pathways [37]. Although all three genes are known to participate in cell senescence, p16 plays a predominant role, with much higher gene expression levels in grade

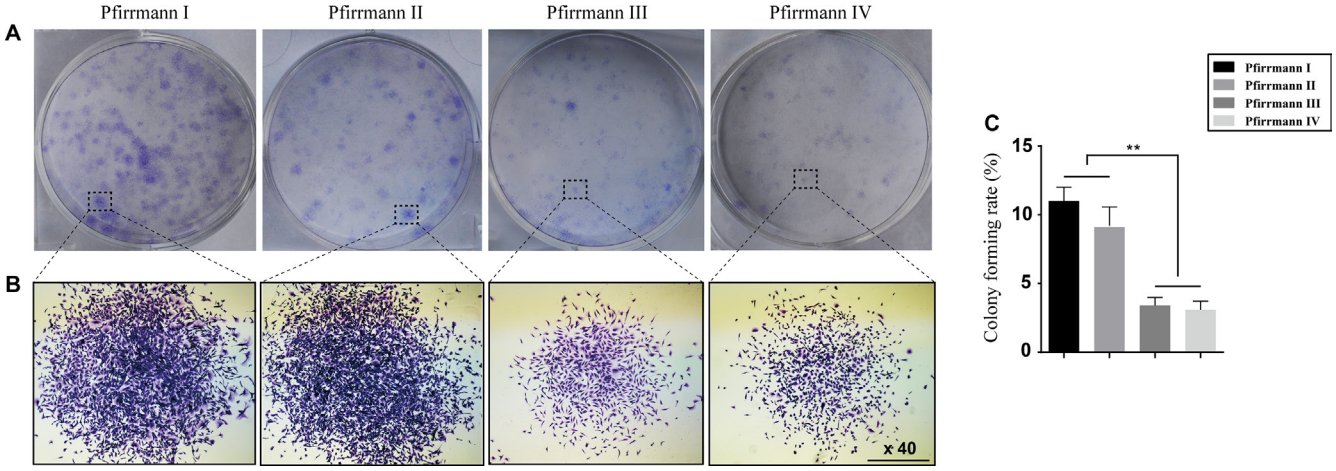

Figure 4: Colony-forming ability of NPPCs from grade I to IV IVDs. (**A** and **B**) Colonies were formed and stained with crystal violet 13 days after initial cell seeding in P3 cells. (**C**) The colony-forming rate of P3 NPPCs gradually declined from grade I to IV, with a marked decline in the colony-forming rate at grade III and IV. $^{**}P < 0.01$ was considered to indicate significant differences between groups.

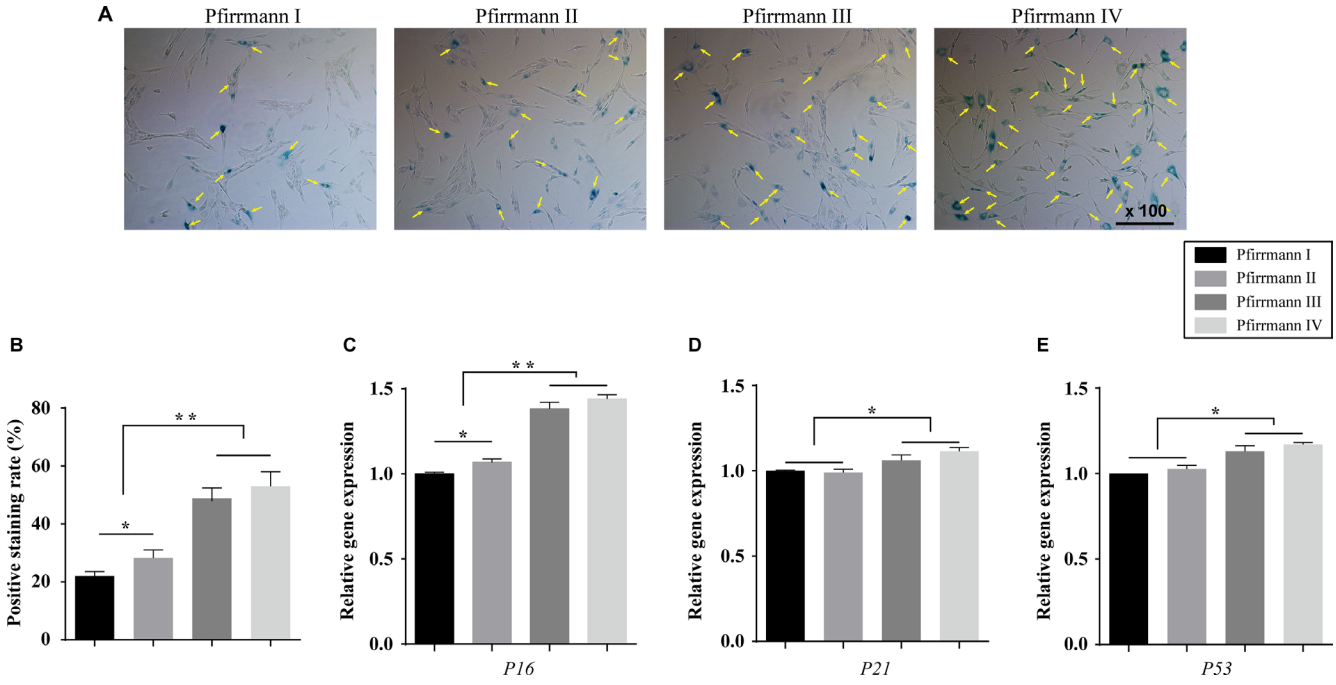

Figure 5: Cellular senescence of NPPCs from grade I to IV IVDs. (**A**) Cell senescence of P9 cells was detected by positive SA-β-gal staining. (**B**) The percentage of SA-β-gal-positive stained cells gradually increased from grades I to IV, with a slightly higher positive rate for grade II ($P < 0.05$, $n = 3$) and a markedly higher rate for grades III and IV than for grade I ($P < 0.01$, $n = 3$). (**C**–**E**) p16, p21 and p53 mRNA levels all slightly increased from grades I to IV, with markedly higher expression in grade III and IV cells ($P < 0.05$, $n = 3$). $^{*}P < 0.05$ and $^{**}P < 0.01$ were considered to indicate significant differences between groups.

III and IV cells. Collectively, the above tests suggested a rapid increase in senescent cells among grade III and IV NPPCs. Given that NPPCs play a crucial role in the maintenance of normal NP tissue homeostasis, the accumulation of senescent cells may reduce the repair and regenerative potential of IDD. Hence, based on these findings, the optimal regeneration window for IVDs may be at grade II.

Migration capacity is another crucial biological characteristic for SCs, facilitating cell targeting to damaged tissue [38]. NPPCs were detected to gradually migrate from the outside niche regions toward the inner part of IVDs as part of regeneration process [39]. In the present study, all four grades of NPPCs possessed varying degrees of migration ability. In wound-healing assays, cells exhibited a declining trend in migration distance from grades I to IV, hinting that migration potential is weakened in degenerated IVDs. In addition, this result also indicated that the decline in migration was due to a decrease in NPPC migration ability rather than to degeneration altering the extracellular matrix in IDD.

Finally, chondrogenic differentiation ability was evaluated using a pellet culture protocol [40]. Cells from grade I to IV IVDs all exhibited chondrocyte differentiation ability, with the GAG/weight and collagen II reflecting chondrogenic ability by ECM accumulation [33]. The results showed that all pellets were intensively positive for Alcian blue staining, with pellet GAG/ weights and collagen II gradually declining with increasing grade. In addition, qPCR assays also showed decreases in the expression of chondrogenic genes (Sox-9and collagen IIα1), with large decreases in grades III and IV. Sox-9 plays an essential role in chondrogenesis and promotes collagen IIα1 and aggrecan gene expression. As aggrecan gene expression was not altered, the decline in chondrogenic ability from grades I to IV may be due to decreasing expression levels of collagen IIα1.

Nevertheless, our study has some limitations. First, NPPCs were obtained from only four Pfirrmann grades (grades I to IV) due to the difficulty of harvesting grade V NP tissue in IDD. Second, the homogeneity of cells derived from the same grade may be affected by various factors, such as age, gender, and segment [41]. Although these differences in these factors were difficult to avoid, they were reduced as much as possible by selecting patients with similar ages and operation segments. In addition, the microenvironment in degenerated IVDs is complex and includes acidic conditions, hypoxia, high osmotic pressure and limited nutrition [28, 42]. These factors are difficult to completely balance and likely differed in the *in vitro* culture medium. In future studies, mimicking the degenerated environment should be taken into consideration. As the present study was conducted *in vitro*, future *in vivo* studies are needed.

In summary, this study harvested NPPCs from Pfirrmann grade I to IV IVDs, which were confirmed as SCs by the standards of the ISCT. NPPCs from grades I to IV IVD exhibited similar cell properties with some differences. From grades I to IV, cell characteristics, including morphology, proliferation, colony formation, migration and chondrogenic ability, gradually decreased, while cell senescence increased. The greatest changes were found between grades II and III in all the above cell properties (Figure 8). Taking all these factors into consideration, grade II IVDs demonstrated the optimal regeneration opportunity, and therefore, grade II NPPCs are the best candidates for endogenous repair of IDD.

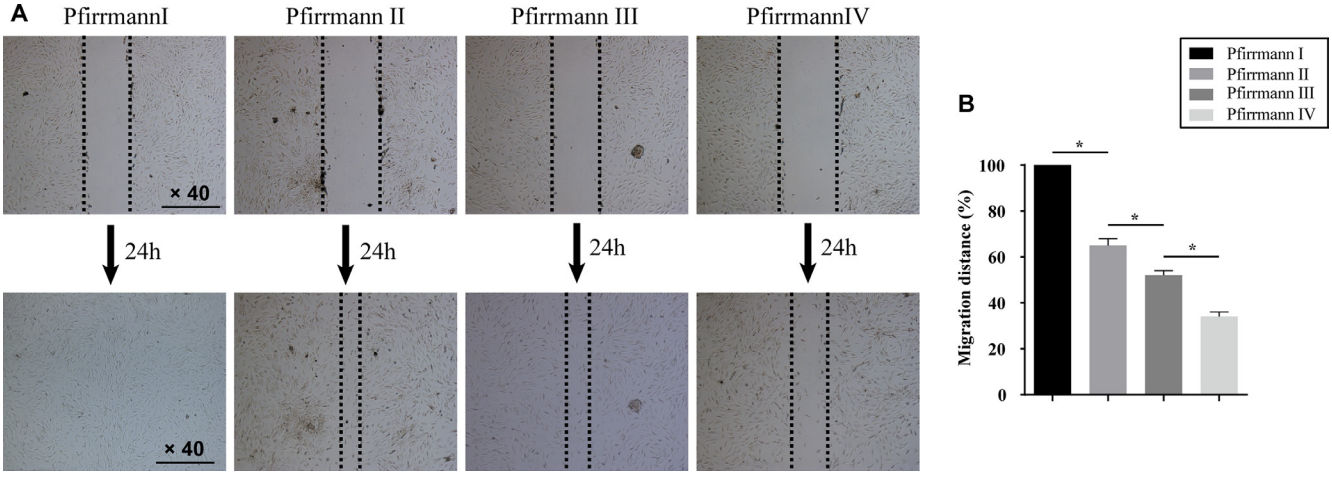

Figure 6: Migration abilities of NPPCs from grade I to IV IVDs. (**A**) Representative examples of the different migration efficiencies of NPPCs are shown. (**B**) Bar graph showing the different migration distance percent of NPPCs, with gradually shorter migration distance observed from grades I to IV ($P < 0.05$, $n = 3$). $^{*}P < 0.05$ was considered to indicate a significant difference between groups.

MATERIALS AND METHODS

Isolation and identification of human NPPCs

NP samples were isolated from 16 patients; the detailed information is shown in Table 1. After the annulus fibrosus and cartilaginous endplates were removed, the NP samples were completely washed at least three times to remove blood tissue. Then, representative photographs of the NP tissues used in this study were obtained and are shown in Figure 1B. The experimental protocols were approved by the Committee of Navy General Hospital (No. 2016-108), and informed consent was obtained from each patient.

The NP samples were collected and immediately transported to a cell culture room under sterile conditions. Next, the NP tissues were mechanically minced into small pieces (< 1 mm^3) and digested with 0.25% collagenase II (Sigma, St. Louis, USA) for 4 h at 37°C in a humidified incubator. The suspended cells were then filtered through a 200-μm mesh filter and centrifuged at 1000 rpm for 5 minutes, followed by two washes with phosphate-buffered

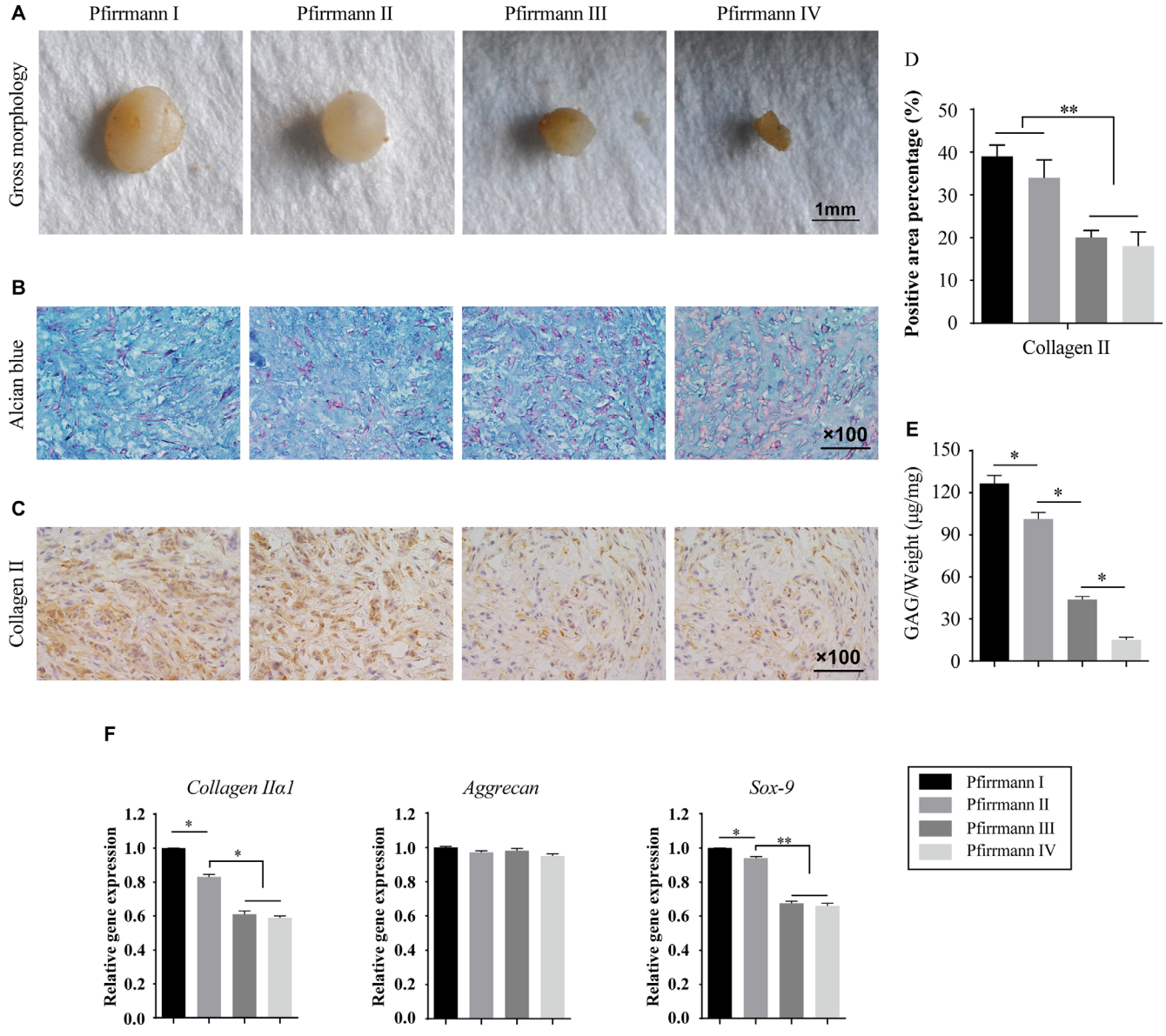

Figure 7: Chondrogenic ability of NPPCs from grade I to IV IVDs. (**A**) The gross morphology of pellets from grade I to IV IVDs after 6 weeks of chondrogenic induction. (**B**) Pellets stained positively for Alcian blue after 6 weeks of chondrogenic induction. (**C**, **D**) Pellets showed positive immunohistochemical staining for collagen II and were quantitatively analyzed after 6 weeks of chondrogenic induction. (**E**) Comparison of pellet GAG content/weight in the four grades, which revealed a significant decrease from grades I to IV ($P < 0.05$, $n = 3$). (**F**) *Collagen IIα1, aggrecan* and *Sox-9* gene expression levels in NPPCs from grade I to IV IVD. after 6 weeks of chondrogenic induction. ($P < 0.05$, $n = 3$). $^{*}P < 0.05$ and $^{**}P < 0.01$ were considered to indicate significant differences between groups.

Table 1: Detailed characteristics of the enrolled patients

Case No.	Diagnosis	Disc level	Pfirrmann grade	Gender	Age (years)
1	Hemivertebra scoliosis	L1-L2	I	F	15
2	lumbar vertebra fracture	T12-L1	I	M	26
3	lumbar vertebra fracture	L2-L3	I	M	49
4	Lumbar disc herniation	L4-L5	II	M	45
5	Lumbar disc herniation	L5-S1	II	F	51
6	Lumbar disc herniation	L4-L5	II	M	46
7	Lumbar disc herniation	L5-S1	II	M	57
8	Lumbar spinal stenosis	L4-L5	III	F	53
9	Lumbar disc herniation	L5-S1	III	M	47
10	Lumbar spinal stenosis	L5-S1	III	M	56
11	Lumbar spinal stenosis	L4-L5	III	F	61
12	Lumbar disc herniation	L4-L5	III	M	45
13	Lumbar spinal stenosis	L5-S1	IV	M	56
14	Lumbar spondylolisthesis	L4-L5	IV	F	49
15	Lumbar spinal stenosis	L4-L5	IV	F	58
16	Lumbar spinal stenosis	L5-S1	IV	M	55

saline (PBS). Finally, the cell pellet was resuspended in DMEM-LG supplemented with 10% FBS and 1% penicillin/streptomycin in a 25-cm^2 cell culture flask at a density of 1×10^5 cells/ml and cultured in a humidified incubator at 37°C with 5% CO_2. As the cells reached 75% confluency, the primary cells were harvested and subcultured at a density of 500 cells/ml in 60-mm tissue culture dishes for colony forming sorting. After 14 days in culture, the colony cells, P1

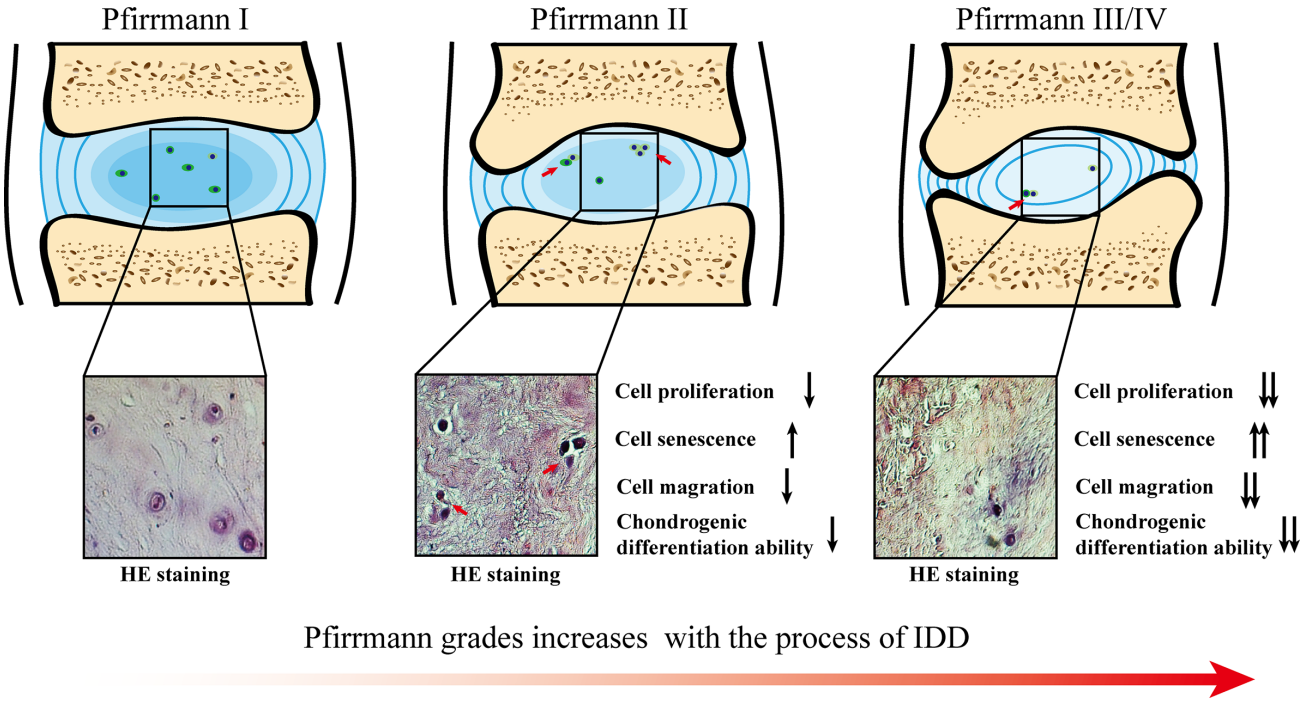

Figure 8: Pathological changes in the cellular properties of NPPCs during the progress of IDD. NPPCs from normal IVDs (Grade I) are in a 'quiescent' state, physiologically maintaining homeostasis of the NP. In early-stage IDD (Grade II), NPPCs become 'active' to repair damaged NP tissue and mainly display cell cluster formation, with decreasing of cell proliferation, cell migration and chondrogenic differentiation abilities and increasing cell senescence. As degeneration progresses (Grades III and IV), the degenerated IVDs finally reach an irreversibly degenerated stage characterized by a major decline in cell function and increased cell senescence. The red arrows indicate endogenous NPPCs.

NPPCs, were harvested with 0.25% trypsin–EDTA (Sigma) for 2 minutes and then subcultured [33]. The cells were gradually passaged, and passage 3 (P3) cells were harvested for identification of phenotype identification. Cells met that the ISCT criteria, positive for CD73, CD90, and CD105 expression (> 95%) and negative for CD34, CD45 and HLA-DR (< 2%), were selected for further experiments.

Flow cytometry identification

P3 cells were harvested in a cell suspension at a concentration of 1×10^6 in 500 µl and transferred to a 1.5-ml centrifuge tube. Next, the cells were incubated in the dark for 30 minutes at 4°C with 5 µL of fluorescein isothiocyanate (FITC)- or phycoerythrin (PE)-conjugated antibodies against CD34, CD105, HLA-DR (Abcam, Cambridge, MA, USA), CD45, CD73, and CD90 (BD Pharmingen, San Diego, CA, USA). The cells were then washed twice with cold PBS and resuspended in 500 ml cold PBS for analysis using a FACSCalibur system (BD, USA) to detect the expression of specific surface markers.

Cell proliferation capacity assay

To measure proliferation capacity, a Cell Counting Kit-8 (CCK-8, Dojindo Laboratories, Japan) and P3 cells were used as described previously [43]. Briefly, 10 µL CCK-8 solution was added to each well of a 96-well plate with 1000 cells per well. After the plate was incubated at 37°C for 1 h, the absorbance was measured at 450 nm using a microplate absorbance reader (BioRad, USA). Cell proliferation was tested on days 1, 3, 5, 7, 9, 11 and 13. A blank 96-well plate was used for the zero setting. All experiments were performed three times for every sample.

Colony-forming assay

To test the colony-forming capability, a colony forming unit-fibroblast (CFU-F) assay was performed. Highly diluted single-cell suspensions with cell densities of 500 cells/ml were plated and cultured for 10 days. The cells were then washed and fixed with 4% paraformaldehyde for 15 minutes. After two rinses with PBS, the cells were stained with 0.1% crystal violet (Keygen Biotech, Nanjing, China) at 4°C, and the colonies were photographed and counted. The colony diameter was measured by the average of two perpendicular diameters. All experiments were performed three times.

Senescence-associated β-galactosidase (SA-β-gal) staining

Cell senescence assays in different Pfirrmann grades were analyzed with a Senescence β-Galactosidase Staining Kit (Beyotime Institute of Biotechnology, China). Briefly, P9 cells were washed with PBS and then fixed in SA-β-gal fixative solution for 15 minutes at room temperature. After three rinses with PBS, the cells were incubated in SA-β-gal working solution (Reagents A, B, C, and X-Gal) overnight at 37°C under an atmosphere without CO_2. Quantification was performed by counting the number of SA-β-gal-positive cells among the total number of cells in three randomly selected visual fields (magnified 200 times) from each culture plate of each sample. For SEM (Inspect S50 FEI, USA) of P3 and P9 cells, all samples were fixed, dehydrated, and coated with platinum. Then, images were obtained with a JEOL scanning electron microscope (Inspect S50 FEI, USA) at 2000× magnification and 15 kV. All experiments were performed three times for each patient.

Wound-healing and cell migration assays

For the wound-healing assay, 1×10^5 P3 cells were seeded into 6-well plates and cultured to 90% confluence. A straight line (mimicking a wound injury) was created using a 20-µl pipette tip. Photomicrographs of the same regions were acquired before and after 24 h of incubation in serum-free FCS DMEM-LG. The migration areas of wound healing were measured and calculated by ImageJ software. For the cell migration assay, 2×10^4 cells in 200 µl serum-free DMEM-LG were added to the upper chamber of a transwell plate with 8-µm pores, and 600 µl DMEM-LG containing 10% FCS was added to the lower chamber. Next, the transwell chamber plates were incubated in a humidified incubator at 37°C in 5% CO_2. After 12 h, the cells on the upper sides of the membranes were carefully removed with a cotton swab, and the cells on the underside of the membranes were fixed and stained with 0.1% crystal violet. After the cells were thoroughly washed, the migrating cells were counted three times for every sample.

Multilineage differentiation tests and chondrogenic differentiation ability assay

The multilineage differentiation potential of P3 NPPCs was determined by osteogenic, adipogenic and chondrogenic differentiation assays. Cells cultured with culture medium served as controls.

For osteogenic differentiation, 2.0×10^4 P3 cells were cultured in human MSC osteogenic differentiation medium (Cyagen Biosciences, Guangzhou, China), which was changed every 3 days. The cells were fixed with 4% formaldehyde and stained with alizarin red (Sigma) for 15 minutes after 21 days in culture.

For adipogenic differentiation, 2.0×10^4 P3 cells in each plate were incubated for 72 h in induction medium A, which was then replaced with maintenance medium B for 24 h. This 96-h induction-maintenance cycle was repeated four times; ultimately, the cells were incubated in maintenance medium B for 7 days. The cells were fixed with 4% formaldehyde and stained with oil red O (Sigma) for 15 minutes, and hematoxylin was used for nuclear staining.

Table 2: Primers used for quantitative real-time polymerase chain reaction

Gene	Forward primers (5′–3′)	Reverse primers (5′-3′)
GAPDH	ACCACAGTCCATGCCATCAC	TCCACCACCCTGTTGCTGTA
Collagen II α1	GGTAAGTGGGGCAAGACTGTTA	TGTTGTTTCTGGGTTCAGGTTT
Sox-9	GCCTCTACTCCACCTTCACCTA	GCTGTGTGTAGACAAGTTGTT
Aggrecan	GTCAGATACCCCATCCACACTC	CATAAAAGACCTCACCCTCCAT
p16	TTCCCCCACTACCGTAAATGT	GCTCACTCCAGAAAACTCCAAC
P21	CTCAAAGGCCCGCTCTACAT	AATGCCCAGCACTCTTAGGAA
P51	CCGCAGTCAGATCCTAGCG	AATCATCCATTGCTTGGGACG

For chondrogenic differentiation, 2.0×10^4 P3 cells were harvested and seeded into multi-well cell culture plates in culture medium. After 24 h, the culture medium was replaced with chondrogenic differentiation medium (Cyagen Biosciences, Guangzhou, China). The cells were treated twice weekly with fresh chondrogenic differentiation medium for 4 weeks. Finally, the cells were rinsed three times with PBS, fixed with 4% paraformaldehyde for 15 minutes at room temperature, washed with PBS, and stained with 1% Alcian blue for 15 minutes.

In addition, chondrogenic differentiation was evaluated with a pellet culture protocol. Cell pellets were generated by centrifuging (1500 rpm) a cell suspension (P3 cells at 5×10^6 cells/ml) in a centrifuge tube. After 3 days of cultivation, the medium was replaced with chondrogenic medium (Cyagen Biosciences, Guangzhou, China) and changed every other day for 4 weeks. The weight and pellet diameter of the cell pellets were recorded. The gene expression levels of collagen IIα1, aggrecan and Sox-9 were tested. All the above outcomes were based on experiments performed in triplicate.

Real-time polymerase chain reaction assay

Total RNA was extracted from P3 cells as described previously [33]. The RT reaction (2 μL) was amplified in quadruplex by real-time PCR (ABI PRISM 7000) in a final volume of 25 μL, using SYBR Green Master Mix reagent (Applied Biosystems, Foster City, CA). The specific primers used for chondrogenic and cell senescence markers are shown in Table 2. GAPDH expression was used to normalize the expression levels of all the genes. For each cDNA sample, the cycle threshold (Ct) value of each target sequence was subtracted from the Ct value of the reference gene. qPCR was performed to compare differences in the expression levels of cell senescence and chondrogenic genes between groups.

Statistical analysis

All quantitative data are presented as the mean ± standard deviation (SD) with no fewer than three replicates for each experimental condition. Differences in group means between the grade I to IV cells were determined using repeated-measures analysis of variance and Fisher's least significant difference post hoc test. The Mann–Whitney *U*-test was also used as a post hoc test. SPSS version 15.0 software (Chicago, Illinois, USA) was used for statistical analysis, and $p < 0.05$ was considered statistically significant.

Abbreviations

IVD: Intervertebral disc; IDD: Intervertebral disc degeneration; NP: Nucleus pulposus; NPPCs: Nucleus pulposus progenitoer cells; ECM: Extracellular matrix; SC: Stem cell; MSCs: Mesenchymal stem cells; ISCT: International Society for Cellular Therapy; FITC: Fluorescein isothiocyanate; PE: Phycoerythrin; CCK-8: Cell Counting Kit-8; CFU-F: Colony forming unit-fibroblast; Ct: Cycle threshold.

Author contributions

LXC, BXD and XHK participated in the design of the study, performed cell culture, microscopy analyses, and imaging detection, and interpreted the of results. LXC, BYW, WDL, and WTY performed the imaging analysis. PSS CS and YJW carried out the histological evaluation and gene detection. HQ participated in the design of the study and reviewed the manuscript. LXC and RDK conceived of the study, participated in the design and coordination of the study, provided financial support, and helped revise the manuscript. All authors read and approved the final manuscript.

CONFLICTS OF INTEREST

The authors declare that they have no competing interests.

FUNDING

This work was supported by the National Natural Science Foundation of China (81472121, 81301579, 81470102).

REFERENCES

1. Ruan D, He Q, Ding Y, Hou L, Li J, Luk KD. Intervertebral disc transplantation in the treatment of degenerative spine disease: a preliminary study. Lancet. 2007; 369:993–999.
2. Li X, Bai X, Wu Y, Ruan D. A valid model for predicting responsible nerve roots in lumbar degenerative disease with diagnostic doubt. BMC musculoskeletal disorders. 2016; 17:128.
3. Leung VY, Aladin DM, Lv F, Tam V, Sun Y, Lau RY, Hung SC, Ngan AH, Tang B, Lim CT, Wu EX, Luk KD, Lu WW, et al. Mesenchymal stem cells reduce intervertebral disc fibrosis and facilitate repair. Stem cells. 2014; 32:2164–2177.
4. Huang YC, Leung VY, Lu WW, Luk KD. The effects of microenvironment in mesenchymal stem cell-based regeneration of intervertebral disc. Spine J. 2013; 13:352–362.
5. Li Z, Peroglio M, Alini M, Grad S. Potential and limitations of intervertebral disc endogenous repair. Curr Stem Cell Res Ther. 2015; 10:329–338.
6. Risbud MV, Guttapalli A, Tsai TT, Lee JY, Danielson KG, Vaccaro AR, Albert TJ, Gazit Z, Gazit D, Shapiro IM. Evidence for skeletal progenitor cells in the degenerate human intervertebral disc. Spine. 2007; 32:2537–2544.
7. Blanco JF, Graciani IF, Sanchez-Guijo FM, Muntion S, Hernandez-Campo P, Santamaria C, Carrancio S, Barbado MV, Cruz G, Gutierrez-Cosio S, Herrero C, San Miguel JF, Brinon JG, del Canizo MC. Isolation and characterization of mesenchymal stromal cells from human degenerated nucleus pulposus: comparison with bone marrow mesenchymal stromal cells from the same subjects. Spine. 2010; 35:2259–2265.
8. Henriksson HB, Svala E, Skioldebrand E, Lindahl A, Brisby H. Support of concept that migrating progenitor cells from stem cell niches contribute to normal regeneration of the adult mammal intervertebral disc: a descriptive study in the New Zealand white rabbit. Spine. 2012; 37:722–732.
9. Navaro Y, Bleich-Kimelman N, Hazanov L, Mironi-Harpaz I, Shachaf Y, Garty S, Smith Y, Pelled G, Gazit D, Seliktar D, Gazit Z. Matrix stiffness determines the fate of nucleus pulposus-derived stem cells. Biomaterials. 2015; 49:68–76.
10. Tao Y, Zhou X, Liang C, Li H, Han B, Li F, Chen Q. TGF-beta3 and IGF-1 synergy ameliorates nucleus pulposus mesenchymal stem cell differentiation towards the nucleus pulposus cell type through MAPK/ERK signaling. Growth factors. 2015:1–11.
11. Vaga S, Brayda-Bruno M, Perona F, Fornari M, Raimondi MT, Petruzzi M, Grava G, Costa F, Caiani EG, Lamartina C. Molecular MR imaging for the evaluation of the effect of dynamic stabilization on lumbar intervertebral discs. Eur Spine J. 2009; 18:40–48.
12. Tao YQ, Liang CZ, Li H, Zhang YJ, Li FC, Chen G, Chen QX. Potential of co-culture of nucleus pulposus mesenchymal stem cells and nucleus pulposus cells in hyperosmotic microenvironment for intervertebral disc regeneration. Cell Biol Int. 2013; 37:826–834.
13. Li H, Tao Y, Liang C, Han B, Li F, Chen G, Chen Q. Influence of hypoxia in the intervertebral disc on the biological behaviors of rat adipose- and nucleus pulposus-derived mesenchymal stem cells. Cells Tissues Organs. 2013; 198:266–277.
14. Han B, Wang HC, Li H, Tao YQ, Liang CZ, Li FC, Chen G, Chen QX. Nucleus pulposus mesenchymal stem cells in acidic conditions mimicking degenerative intervertebral discs give better performance than adipose tissue-derived mesenchymal stem cells. Cells Tissues Organs. 2014; 199:342–352.
15. Sakai D, Nakamura Y, Nakai T, Mishima T, Kato S, Grad S, Alini M, Risbud MV, Chan D, Cheah KS, Yamamura K, Masuda K, Okano H, et al. Exhaustion of nucleus pulposus progenitor cells with ageing and degeneration of the intervertebral disc. Nat Commun. 2012; 3:1264.
16. Grad S, Peroglio M, Li Z, Alini M. Endogenous cell homing for intervertebral disk regeneration. J Am Acad Orthop Surg. 2015; 23:264–266.
17. Li XC, Wu YH, Bai XD, Ji W, Guo ZM, Wang CF, He Q, Ruan DK. BMP7-Based Functionalized Self-Assembling Peptides Protect Nucleus Pulposus-Derived Stem Cells From Apoptosis *In Vitro*. Tissue Eng Part A. 2016; 22:1218–1228.
18. Zhao Y, Jia Z, Huang S, Wu Y, Liu L, Lin L, Wang D, He Q, Ruan D. Age-Related Changes in Nucleus Pulposus Mesenchymal Stem Cells: An *In Vitro* Study in Rats. Stem Cells Int. 2017; 2017:6761572.
19. Shen Q, Zhang L, Chai B, Ma X. Isolation and characterization of mesenchymal stem-like cells from human nucleus pulposus tissue. Sci China Life Sci. 2015; 58:509–511.
20. Sakai D, Andersson GB. Stem cell therapy for intervertebral disc regeneration: obstacles and solutions. Nat Rev Rheumatol. 2015; 11:243–256.
21. Vadala G, Russo F, Ambrosio L, Loppini M, Denaro V. Stem cells sources for intervertebral disc regeneration. World J Stem Cells. 2016; 8:185–201.
22. Krock E, Rosenzweig DH, Haglund L. The Inflammatory Milieu of the Degenerate Disc: Is Mesenchymal Stem Cell-based Therapy for Intervertebral Disc Repair a Feasible Approach? Curr Stem Cell Res Ther. 2015; 10:317–328.
23. Erwin WM, Islam D, Eftekarpour E, Inman RD, Karim MZ, Fehlings MG. Intervertebral disc-derived stem cells: implications for regenerative medicine and neural repair. Spine. 2013; 38:211–216.
24. Shi R, Wang F, Hong X, Wang YT, Bao JP, Cai F, Wu XT. The presence of stem cells in potential stem cell niches of the intervertebral disc region: an *in vitro* study on rats. Eur Spine J. 2015; 24:2411–2424.
25. Wang H, Zhou Y, Chu TW, Li CQ, Wang J, Zhang ZF, Huang B. Distinguishing characteristics of stem cells

derived from different anatomical regions of human degenerated intervertebral discs. Eur Spine J. 2016; 25:2691–2704.

26. Liu J, Tao H, Shen C, Liu X, Wang H, Dong F, Zhang R, Li J, Ge P, Song P, Zhang H, Xu P. Biological behavior of human nucleus pulposus mesenchymal stem cells in response to changes in the acidic environment during intervertebral disc degeneration. Stem Cells Dev. 2017; 26:901–911.
27. Richardson SM, Kalamegam G, Pushparaj PN, Matta C, Memic A, Khademhosseini A, Mobasheri R, Poletti FL, Hoyland JA, Mobasheri A. Mesenchymal stem cells in regenerative medicine: Focus on articular cartilage and intervertebral disc regeneration. Methods. 2016; 99:69–80.
28. Huang YC, Leung VY, Lu WW, Luk KD. The effects of microenvironment in mesenchymal stem cell-based regeneration of intervertebral disc. Spine J. 2013; 13:352–362.
29. Dumitru I, Neitz A, Alfonso J, Monyer H. Diazepam Binding Inhibitor Promotes Stem Cell Expansion Controlling Environment-Dependent Neurogenesis. Neuron. 2017; 94:125–137.e125.
30. Wang F, Shi R, Cai F, Wang YT, Wu XT. Stem Cell Approaches to Intervertebral Disc Regeneration: Obstacles from the Disc Microenvironment. Stem Cells Dev. 2015; 24:2479–2495.
31. Ohnishi T, Sudo H, Tsujimoto T, Iwasaki N. Age-related spontaneous lumbar intervertebral disc degeneration in a mouse model. J Orthop Res. 2017 Jun 20. https://doi.org/10.1002/jor.23634 [Epub ahead of print].
32. Li D, Yue J, Jiang L, Huang Y, Sun J, Wu Y. Correlation Between Expression of High Temperature Requirement Serine Protease A1 (HtrA1) in Nucleus Pulposus and T2 Value of Magnetic Resonance Imaging. Med Sci Monit. 2017; 23:1940–1946.
33. Liu S, Liang H, Lee SM, Li Z, Zhang J, Fei Q. Isolation and identification of stem cells from degenerated human intervertebral discs and their migration characteristics. Acta Biochim Biophys Sin (Shanghai). 2016; 49:101–109.
34. Dominici M, Le Blanc K, Mueller I, Slaper-Cortenbach I, Marini F, Krause D, Deans R, Keating A, Prockop D, Horwitz E. Minimal criteria for defining multipotent mesenchymal stromal cells. The International Society for Cellular Therapy position statement. Cytotherapy. 2006; 8:315–317.
35. Wehling N, Palmer GD, Pilapil C, Liu F, Wells JW, Müller PE, Evans CH, Porter RM. Interleukin-1β and tumor necrosis factor α inhibit chondrogenesis by human mesenchymal stem cells through NF-κB-dependent pathways. Arthritis Rheum. 2009; 60:801–812.
36. Chen FM, Wu LA, Zhang M, Zhang R, Sun HH. Homing of endogenous stem/progenitor cells for *in situ* tissue regeneration: Promises, strategies, and translational perspectives. Biomaterials. 2011; 32:3189–3209.
37. Li C, Wei GJ, Xu L, Rong JS, Tao SQ, Wang YS. The involvement of senescence induced by the telomere shortness in the decline of osteogenic differentiation in BMSCs. Eur Rev Med Pharmacol Sci. 2017; 21:1117–1124.
38. Li L, Jiang J. Regulatory factors of mesenchymal stem cell migration into injured tissues and their signal transduction mechanisms. Front Med. 2011; 5:33–39.
39. Zhang H, Zhang L, Chen L, Li W, Li F, Chen Q. Stromal cell-derived factor-1 and its receptor CXCR4 are upregulated expression in degenerated intervertebral discs. Int J Med Sci. 2014; 11:240–245.
40. Liu LT, Huang B, Li CQ, Zhuang Y, Wang J, Zhou Y. Characteristics of stem cells derived from the degenerated human intervertebral disc cartilage endplate. PloS one. 2011; 6:e26285.
41. Mizrahi O, Sheyn D, Tawackoli W, Ben-David S, Su S, Li N, Oh A, Bae H, Gazit D, Gazit Z. Nucleus pulposus degeneration alters properties of resident progenitor cells. Spine J. 2013; 13:803–814.
42. Bibby SR, Jones DA, Ripley RM, Urban JP. Metabolism of the intervertebral disc: effects of low levels of oxygen, glucose, and pH on rates of energy metabolism of bovine nucleus pulposus cells. Spine. 2005; 30:487–496.
43. Bai XD, Li XC, Chen JH, Guo ZM, Hou LS, Wang DL, He Q, Ruan DK. Coculture with Partial Digestion Notochordal Cell-Rich Nucleus Pulposus Tissue Activates Degenerative Human Nucleus Pulposus Cells. Tissue Eng Part A. 2017; 23:837–846.